Effect of tempering on thermal analysis of Al-Ti-Si alloy and its composites

Rana Afif Anaee, Wafaa Mahdi Salih, Ban Farhan Dawood

Materials Engineering Department, University of Technology

E-mail: Dr.rana_afif@yahoo.com

Abstract

The investigation of the effect of tempering on thermal analysis of Al-Ti-Si alloy and its composites with MgO and SiC particles was performed. Thermal analysis was performed before and after tempering by DSC scan. Optical microscopy was used to identify the phases and precipitations that may be formed in base alloy and composites. X-ray diffraction test indicated that the Al_3Ti is the main phase in Al-Ti-Si alloy in addition to form $Al_5Ti_7Si_{12}$ phase. Some chemical reactions can be occurred between reinforcements and matrix such as $MgO.Al_2O_3$ in Al-Ti/MgO, and Al_4C_3 and $Al(OH)_3$ in Al-Ti/SiC composite. X-ray florescence technique is used to investigate the chemical composition of the fabricated specimens. Heat treatment (Tempering) changes the microstructure of base alloy and its composites which was assessed by DSC scan. Generally, three main peaks appeared in DSC represented by GP zone, S phase (precipitations) and dissolution of phases or precipitations. After tempering, composite with SiC particles showed better results than base alloy and composite with MgO. Since the optical microscopy revealed reforming the stable phase Al_3Ti with evaporation some gases from composite. DSC analysis showed the stability of composite with SiC was up to 270^oC.

Key words

DSC, Al-Ti-Si alloy, Composite, SiC, MgO, Al_3Ti phase, $Al_5Ti_7Si1_2$.

Article info.

Received: May. 2016
Accepted: Jun. 2016
Published: Dec. 2016

تأثير المراجعة على التحلل الحراري لسبيكة المنيوم – تيتانيوم – سليكون والمواد المتراكبة العائدة لها

رنــا عفيف مجيد، وفــاء مهدي صالح، بان فرحان داود

قسم هندسة المواد، الجامعة التكنولوجية

الخلاصة

لقد تم الكشف عن تأثير المراجعة على التحليل الحراري لسبيكة المنيوم – تيتانيوم – سليكون مع مواده المتراكبة المدعمة باوكسيد المغنيسيوم وكاربيد السليكون بنسبة وزنية 1% من خلال فحص المسعر التفاضلي الحراري. اجري فحص البنية بالمجهر البصري لتشخيص الاطوار المتكونة في السبيكة الاساس والمواد المتراكبة المدعمة وقد اثبت فحص الحيود بالاشعة السينية تكون الطور الرئيسي Al_3Ti بالاضافة الى تكوين الطور $Al_5Ti_7Si_{12}$ بالاضافة الى اطور اخرى تتكون ضمن المواد المتراكبة مثل $MgO.Al_2O_3$ و Al_4C_3 و $Al(OH)_3$ واطوار اخرى. ان المعاملة الحرارية تغير من تفاعلات التبلور والانصهار الظاهرة في فحص التحلل الحراري باستخدام المسعر الماسح التفاضلي. ان قمم التبلور الرئيسية الظاهرة في فحص التحلل الحراري هي ظهور طبقة GP وقمة الطور البيني S وقمة الاطوار غير المتماسكة. ان المادة المتراكبة المدعمة بدقائق كاربيد السليكون تظهر من خلال الفحص بالمسعر الماسح التفاضلي استقراراً حرارياً واضحاً الى حد 270 درجة مئوية.

Introduction

Composites are materials in which two phases are combined, usually with strong interfaces between them. The current and potential applications of aluminum based composites are concentrated on three specific areas: the automotive industry, the aerospace sector and the leisure market. However, interest is also growing in the field of mechanical applications (mostly for wear resistant or high precision applications) and in the field of electrical and electronic applications [1, 2].

Differential scanning calorimetry (DSC) and isothermal calorimetry have been applied extensively to the analysis of light metals, especially Al based alloys. Isothermal calorimetry and differential scanning calorimetry are used for analysis of solid state reactions, such as precipitation, homogenization, devitrivication, recrystallisation; and solid–liquid reactions.

Some authors highlighted fabrication and studying properties of Al-Ti alloy [3-7] and there are many researches focus thermal analysis of aluminum alloys and aluminum matrix composites [8-13].

This work aims to study the effect of tempering on Al-Ti-Si alloy and reinforced by MgO and SiC through optical microscopy and differential scanning calorimetry to identify the interaction between reinforcements and matrix.

Experimental procedure

Preparation of specimens

Al wires and Ti powder was used to fabricate the base alloy and its composites with 1 wt% of MgO or SiC by stir casting technique. Al wires and other powders were used, where the particle size of Ti was 165 μm, while was 53 and 20 μm for MgO and SiC respectively. For the production of composite specimens, matrix material Al was put in the crucible and the melting process was started and continued until the temperature of the liquid matrix reached 700°C. Stirring apparatus was immersed in the liquid metal and stirring was started. The appropriate amount of Ti, Si then MgO and SiC with 1 wt.% was added in the liquid metal by a funnel during the stirring process. After the addition of reinforcement to liquid matrix, the mixture was stirred for about 4 min at 500 rpm in order to allow homogeneous distribution of MgO or SiC particles in the mixture. When stirring was completed, the crucible was taken out of the furnace, the molten liquid was poured in to steel containers of 20 mm diameter and 170 mm height and was allowed to cool down to room temperature. The chemical composition of base alloy is shown in Table 1 which obtained by SpectroMAX technique (AMETEK).

The specimens were cut into cylindrical shapes for characterization and thermal conductivity test with dimensions of 20 mm diameter and 4 mm high. Grinding and polishing was done with emery papers 220, 400, 500, 800, and 1000 mesh grit and then rinsed with acetone. The specimens were etched with Killers solution (2 ml HF +3 ml HCl + 5 ml HNO_3 + 190 ml H_2O) as etchant for 10-30 sec for optical examination.

X-Ray diffraction

XRD was carried out by X-Ray Diffractometer, Model: XRD-6000 with Cu-Kά as target at voltage= 40 (kV) and current= 30 (mA). While EDS was done by Scanning Electron Microscope (SEM), Model: Tescan VEGA 3 SB with Electron Gun: Tungsten Heated Filament and Voltage 200 (V) to 30 (kV).

Optical microscopy

The microstructure evolution was investigated by means of optical microscope using (BEL photonics) microscope.

Differential scanning calorimetry (DSC)

The differential scanning calorimetry analysis was carried out using the 131EVO differential thermal analyzer from SETARAM. Each of the specimens was put in the sample holder, and the sample and an inert reference material were made to undergo identical thermal cycles by heating to a temperature of 500^{o}C and then cooling to room temperature at a rate of 10 ^{o}C.min^{-1}. The differential temperature and temperature signals were then recorded and the plot of heat flow against temperature was obtained by using a computerized data processing unit. Heat capacities ΔC_p and T_g also be calculated.

Results and discussion

XRD Pattern

Fig.1 shows the XRD pattern of base alloy. This figure indicates the presence of a main peak for Al_3Ti phase. In Al-Ti binary alloys according to JCPDS card (26-0038) in addition to appear AlTi (JCPDS card 05-0678) and Al_2Ti phase (JCPDS card 42-1136). According to the chemical composition of base alloy, can be seen copper as impurities in alloy. Therefore, $Al_{0.67}Ti_{0.25}Cu_{0.08}$ (JCPDS card 44-1263) also are present in XRD pattern.

The chemical composition of base alloy indicates the presence of phosphor, this lead to form Ti_xP_y phases such as Ti_5P_3 (JCPDS card 45-0888) and Ti_4P_3 (JCPDS card 22-0944). These phases and intermetallic compounds overlapped to obtain intensities at 2θ of 38.5, 44.8 and 78.3^{o}.

Table: 1 Chemical composition of base alloy.

Metal	*P*	*Ti*	*Si*	*Cu*	*S*	*Fe*	*Pb*	*Zr*	*Al*
Wt%	3.45	4.1	3.50	2.26	1.15	1.92	0.3	0.065	82.9

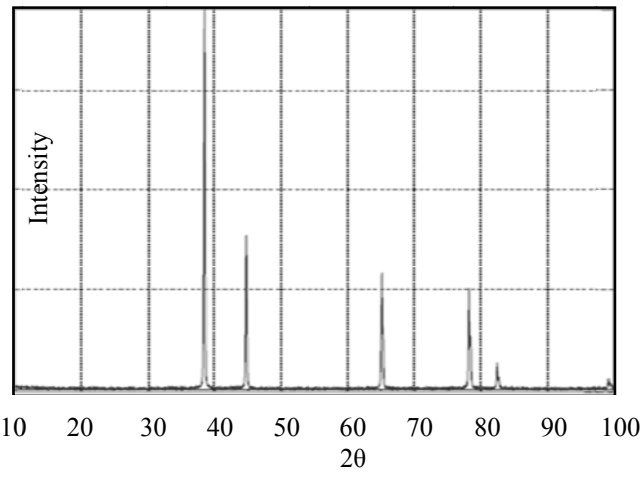

2θ Measured	Intensity	h	k	l
38.5709	100	1	1	1
44.8228	48	2	0	0
78.3197	27	3	1	1

Fig. 1: XRD of fabricated base alloy.

Optical examination

Fig.2 shows optical microscopies of untreated Al-Ti alloy, Al-Ti/1%MgO and Al-Ti/1%SiC composites. The examination of microstructure for base alloy indicates the formation of Al_3Ti phase within Al matrix; this phase describes the particulates as "star-like"

and/or "petal-like" in appearance. Petal-like Al_3Ti particles in α-Al solid solution are shown in Fig. 2 of base alloy are produce according to following reaction:

$Al_{(l)} + Al_3Ti_{(crys)} \rightarrow$ α-Al (*Alloy solid solution)* (1)

Al_3Ti crystals act as nuclei for grains to grow. Multiple nucleations of averagely eight sites may occur on each particle. The structure examination also shows a flake-like structure which is due to $Al_5Ti_7Si_{12}$ phase [8-13].

The addition of reinforcements (MgO and SiC) seems to proceed by diffusion in liquid state as shown in Figs. 2(b and c). The reinforcement material MgO was generally distributed homogeneously as shown in Fig.2b. This situation can be clarified by precipitation of reinforcement during the cooling of liquid mixture due to its higher specific gravity than that of the matrix material Al [14]. There is a lower chance or lower amount of Al_3Ti phase form in presence of MgO in Al-Ti alloy because most of Al are react with oxygen and converting to Al_2O_3 During the casting. At the same time, the aluminum content oxidizes and then reacts with MgO to form a non stoichiometric reaction:

$MgO_{(s)} + Al_2O_{3(s)} \rightarrow MgO.Al_2O_{3(s)}$ (ΔG=-25.365 kJ/mol) (2)

Non-homogenization of SiC particles in Al matrix can be observed in the microstructure of 1 wt.% SiC reinforced aluminum matrix composite as shown in Fig.2c. Some places in Al matrix can be identified without SiC reinforcing particles. Porosities were observed in all microstructures. This was because when SiC particles were added in the melt during casting, it introduced air in the melt entrapped between the particles.

During the fabrication of Al/SiC composite the major problem is the formation of the Al_4C_3 phase at the Al/SiC interface as shown in Fig. 2c, because the SiC is thermodynamically unstable in the Al melt. This brittle reactant Al_4C_3 forms agglomerates at the interface leading to degradation of the composite strength, modulus and corrosion [15, 16]. When processing Al/SiC composites with the metal in molten state is that liquid aluminum tends to attack SiC according to the following reaction:

$4Al_{(l)} + 3SiC_{(s)} \leftrightarrow Al_4C_{3(s)} + 3Si_{(in\ l\ Al)}$ (3)

This reaction is thermodynamically possible because that the standard free energy change for this reaction is negative, and Al_4C_3 and Si are the two major interfacial reaction products. The migration of carbon atoms (exchange of atoms) is involved in a chemical reaction, leading to wettability and bonding improvement.

The Al_4C_3 compound has deleterious effects within the composite because, firstly, as a brittle phase degrades the mechanical properties, and secondly, it reacts with water or with moisture in the ambient, debilitating even more the composite, according to the following reactions:

$Al_4C_{3(s)} + 18H_2O_{(l)} \rightarrow 4Al(OH)_{3(s)} + 3CO_{2(g)} + 12H_{2(g)}$ (ΔG=-1746 kJ/mol) (4)

Some SiC particles in the composites might oxidize during heating, and, then, SiO_2 film forms around the particle surface [17].

Fig.3 shows the microstructure examination of Al-Ti alloy and its composites with 1% MgO and 1%SiC respectively after tempering. From these images, can be seen that Al_3Ti phase is growing up and breaking up into smaller parts. This process is continuing with increasing of the

solution heat treatment time. The titanium particles is going into the matrix [18].

Heat treatments indicate the reduction of the presence and size of the intermetallic precipitations (MgO, SiC) because the heat treatment performed the precipitations get dissolved in the solid solution in the quenching process in base alloy.

Because the reaction (2) can take place, the tempered Al-4Ti/1%MgO image shows the presence of MgO particles in addition to a plate-like structure. While in Al-4Ti/1% SiC composite image, can be seen that the more spontaneous reaction (4) leads to form Al_3Ti phase within Al matrix after tempering.

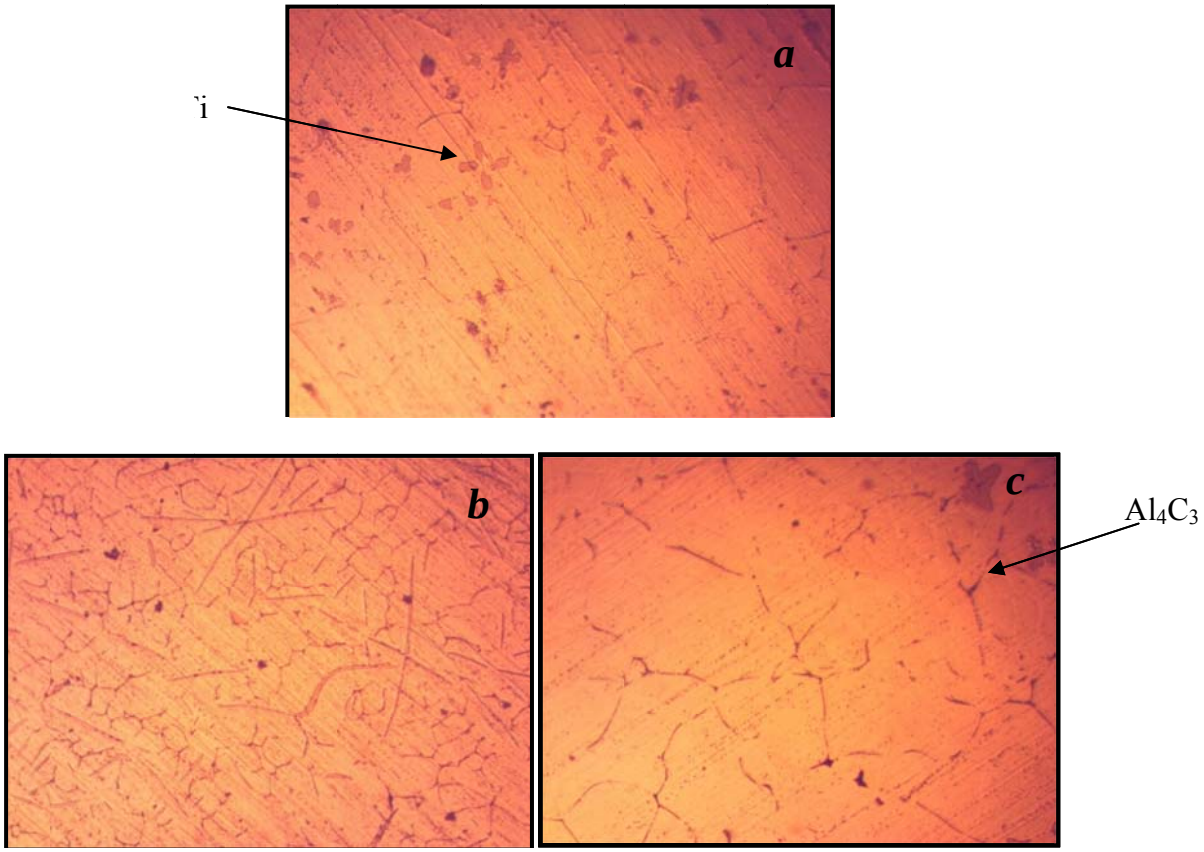

Fig. 2: Optical microscopy of untreated Al-Ti composite at magnification 20X; (a) Al-alloy, (b) Al-alloy/1%MgO, and (c) Al-alloy/1%SiC.

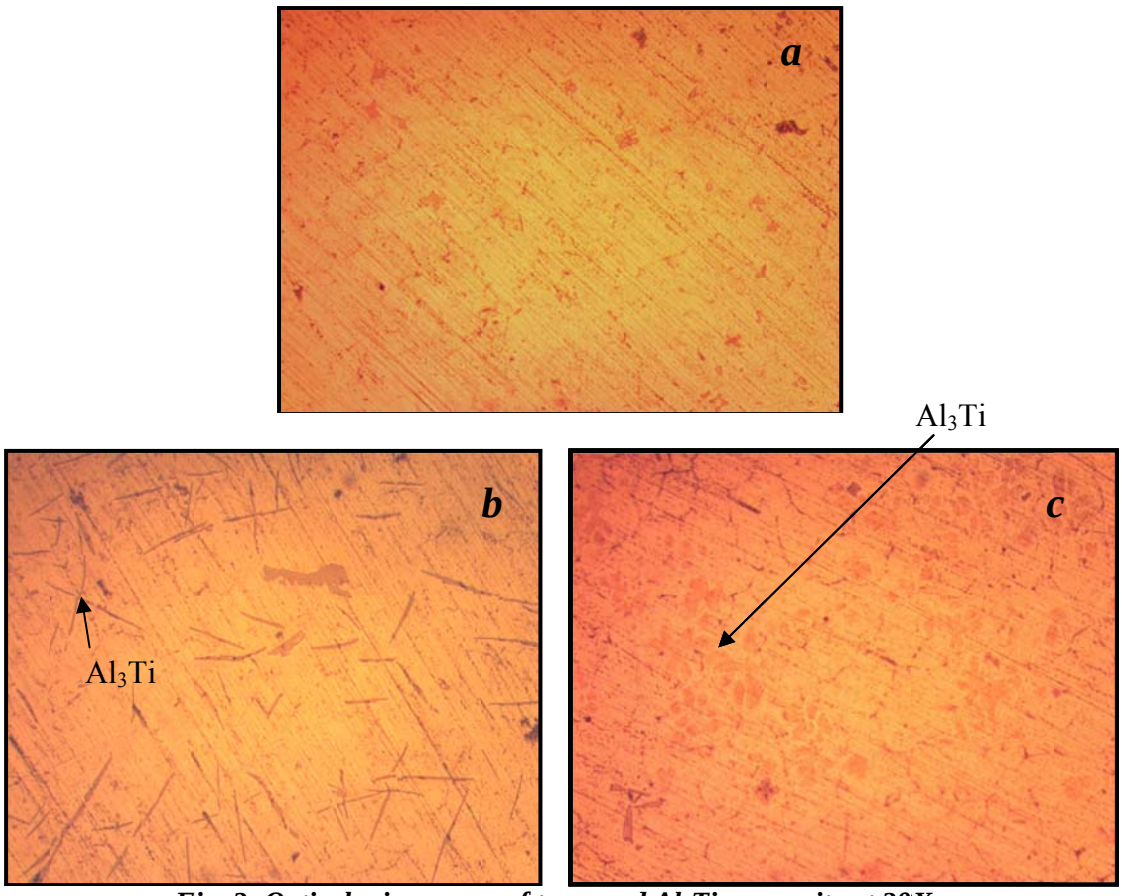

Fig. 3: Optical microscopy of tempered Al-Ti composite at 20X; (a) Al-alloy, (b) Al-alloy/1%MgO, and (c) Al-alloy/1%SiC.

Thermal analysis

DSC analysis is an effective technique to provide a rapid assessment of the temperature range for dissolution of soluble phases as well as providing the onset temperature of incipient melting. The heat effect due to the dissolution of precipitate phases during DSC experiments can be analyzed to yield data on the solving of the phases, even if those phases are metastable.

Fig.4 shows DSC scan of untreated Al-Ti-Si alloy. Peak I at 78.9°C is due to GP zone, since a large number of very small solute-rich clusters form during the early stages of the manufacturing process that are completely coherent, these solute-rich regions will differ somewhat from that of the lattice, strains occur in the lattice regions around the clusters. These regions that are distorted by the clusters are referred to as Guinier-Preston zones. This GP (or δ˝ phase) is dissolves up to ≈ 260°C.

Peak II at 284.4°C ascribed to the precipitations which usually nucleate at dislocations, this peak also refer to produce S/semicoherent phase. These precipitations may be represented by AlTi, Al_2Ti, $Al_{0.67}Ti_{0.25}Cu_{0.08}$ and $Al_5Ti_7Si_{12}$ that appear in structure examination. After that, the melting of these precipitations can occur and continuous up to peak III at ≈ 410°C.

The heat treatment (tempering) led to endothermic melting process at ≈30°C, since the condensed vacancies dissociate with temperature rise and anneal out through the free surface in the material as labeled by peak I and shown in Fig.5. GP zones reformed again (peak II) due to the cluster of different phases and then undergo the dissolution at peak III. S intermetallic

phases appear at exothermic peak marked by IV in Fig.5 that dissolve again at peak V to form incoherent phases at more exothermic peak VI after breaking up Al_3Ti phase as illustrated in optical microscopy.

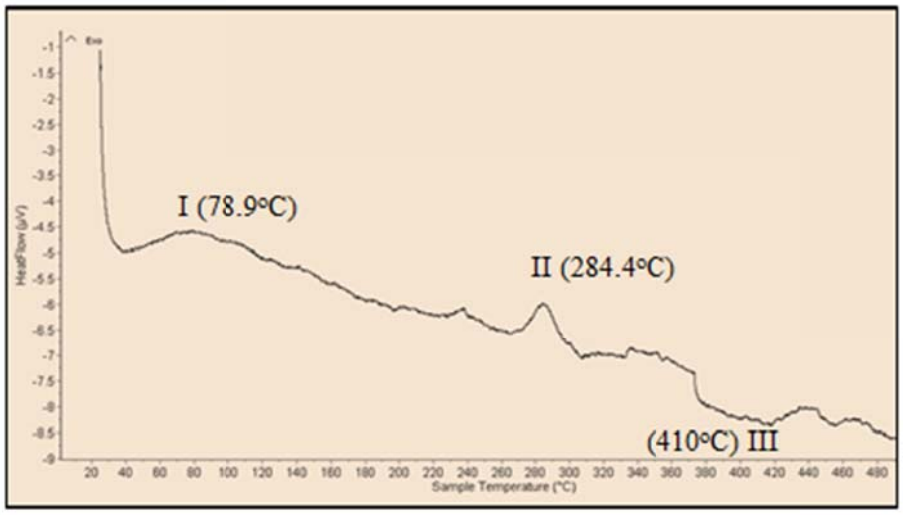

Fig. 4: DSC analysis of untreated Al-Ti alloy.

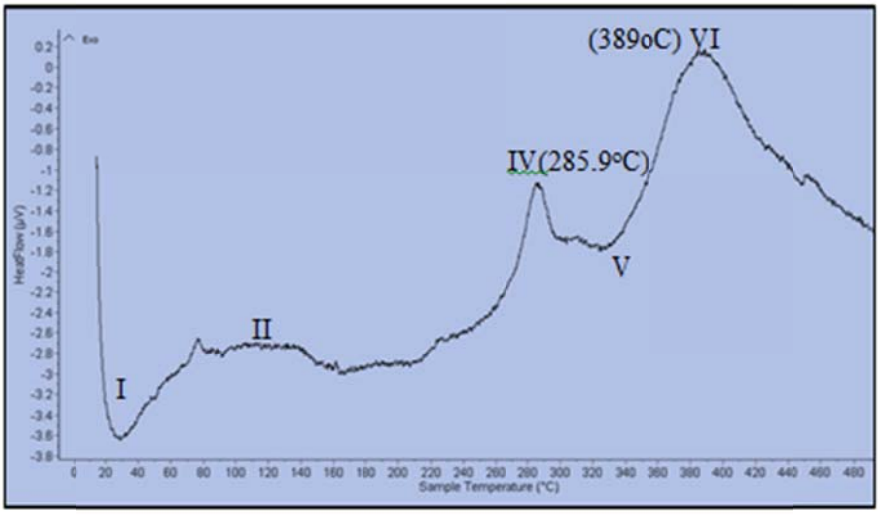

Fig. 5: DSC analysis of tempered Al-4Ti alloy.

The DSC scan of untreated and tempered of Al/1%MgO composite is shown in Fig. 6 and 7 respectively. This scan shows the formation of GP zones followed by dissolution (Peak I in each figure). Peak II is due to formation S intermetallic compounds which become endothermic after heat treatment. These compounds are dissolved at peak III. Peak IV represents the formation of incoherent equilibrium phases. Some surface reactions occur in untreated composite (peak V) such as formation $MgO.Al_2O_3$ according to reaction (2). These surface reactions are disappearing after tempering. The presence of MgO particles in composite lead to inhibiting some reactions in metallic matrix. All peaks after tempering were shifted to lower temperatures.

Figs. 8 and 9 indicate DSC scan of composite with SiC. Peak I in two figures is attributed to melting reactions especially the decomposition

of SiC, these reactions followed by formation GP zone which marked as peak II. Then this zone undergoes dissolution at peak III. Peak IV represented by form S intermetallic phases followed by sharp dissolution especially after tempering due to degassing and extruding, i.e. CO_2 and H_2 were left the material. Even methan gas according to the following reaction may be leaving the composite after heat treatment.

$$Al_4C_{(s)} + 12H_2O_{(l)} \rightarrow 4Al(OH)_{3(s)} + 3CH_{4(g)} \quad (\Delta G=-1847 \text{ kJ/mol}) \qquad (5)$$

Generally, the crystallization and melting peaks became endothermic with very little change in temperature range.

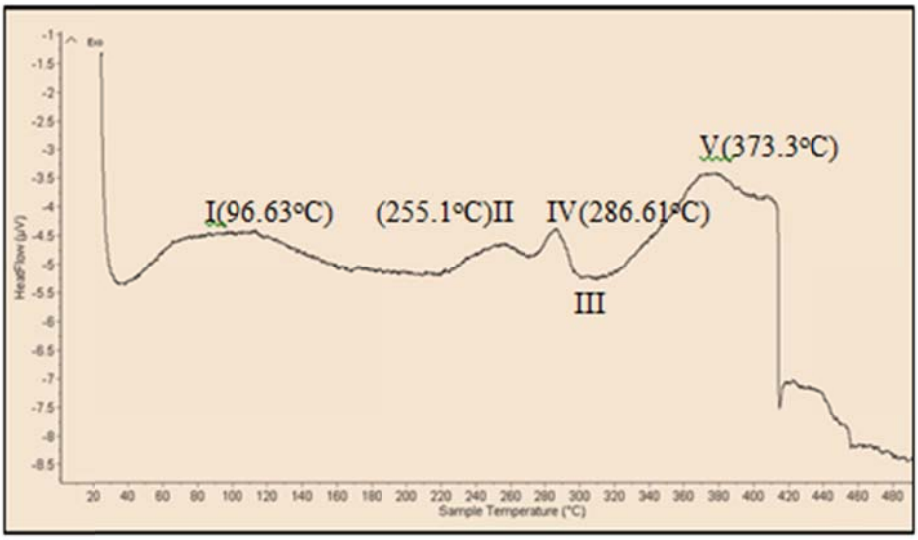

Fig. 6: DSC analysis of untreated Al-Ti/1%MgO composite.

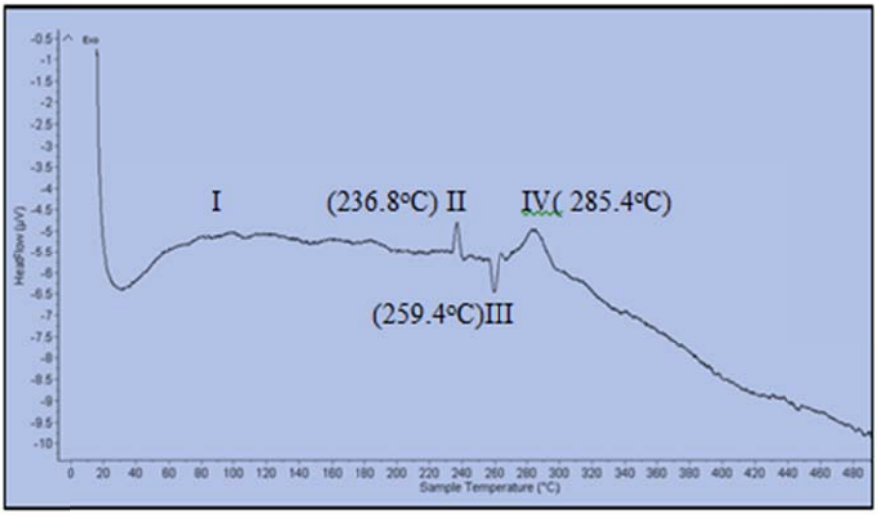

Fig. 7: DSC analysis of tempered Al-Ti/1%MgO composite.

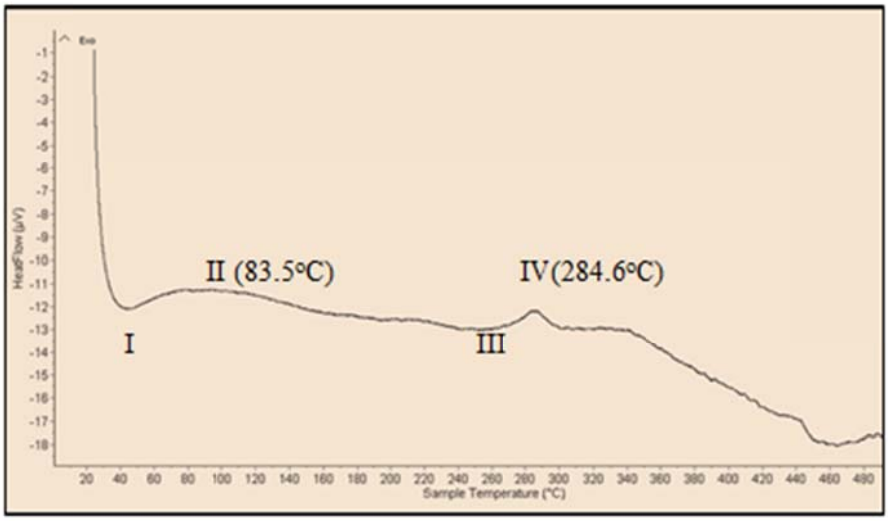

Fig. 8: DSC analysis of untreated Al-Ti/1%SiC composite.

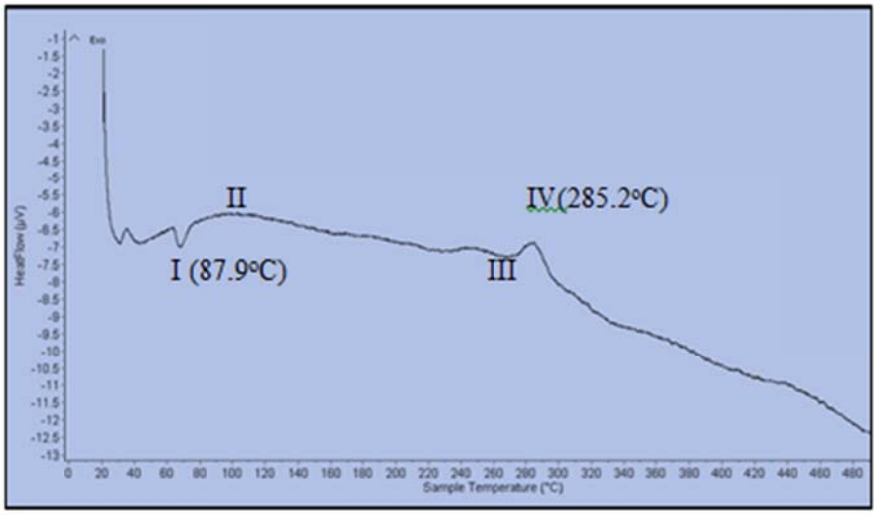

Fig. 9: DSC analysis of tempered Al-Ti/1%SiC composite.

Conclusion

Characterization the role of reinforcing by 1 wt% of MgO and SiC has been investigated by optical microscopy and DSC analysis. The optical microscopy showed the formation of Al_3Ti phase in base alloy (Al-Ti-Si) which broken up with heat treatment in addition to form some phases between metallic materials as impurities in base alloy. The presence of MgO and SiC particles lead to take place many reactions at interfaces and within solid solution of matrix. MgO particles led to precipitate $MgO.Al_2O_3$ with change in free energy higher than that showed between SiC and matrix. SiC particles react with Al to form Al_4C_3 which undergo many reactions to produce gases that may be left the matrix through tempering. DSC analysis showed that a composite with SiC thermally more stable than base alloy and composite with MgO because it was gave lower crystallization and melting peaks.

References

[1] Nikhil V Nayak, Journal of Scientific and Research Publications, 4, 9, September (2014) 1-10.

[2] M. Vukcevic and K.Delijic, Materiali in Tehnologue, 36, (2002) 101-105.

[3] L.A. Dobrzański, K. Labisz, A. Olsen, Journal of Achievements in Materials and Manufacturing Engineering, 26, 2, February 2008.
[4] M. A. Doheim, A. M. Omran, A. Abdel-Gwad, Journal of Engineering Sciences, Assiut University, 36, 2 (2008) 471-481.
[5] L.A. Dobrzański, K. Labisz, R. Maniara, A. Olsen, Journal of Achievements in Materials and Manufacturing Engineering, 37, 2 December (2009).
[6] Segun Isaac Talabi, Samson Oluropo Adeosun, Abdulganiyu Funsho Alabi, Ishaq Na'Allah Aremu, Sulaiman Abdulkareem, International Journal of Metals, Article ID 127106, (2013) 1- 4.
[8] W.F. Miao and D.E. Laughlin, Scripta Materialia, 40, 7 (1999) 873–878.
[9] N. Afify, A. Gaber, A. M. Abousehly, Y. M. Abou Deif, Materials Transactions, 51, 2 (2010) 317-320.
[10] Maja Vončina, Anton Smolej, Jožef Medved, Primož Mrvar, Rok Barbič, Materials and Geoenvironment, 57, 3 (2010) 295–304.
[11] S. I. Določitev and D. Al-zlitinah, RMZ– Materials and Geoenvironment, 57, 3 (2010) 295-304.
[12] O. A. Alo, L. E. Umoru, J. A. Ajao, K. M. Oluwasegun, Journal of Minerals & Materials Characterization & Engineering, 11, 2 (2012) 159-168.
[13] Maher Mounib, Matteo Pavese, Claudio Badini, Williams Lefebvre, Hajo Dieringa, Advances in Materials Science and Engineering, Article ID 476079 (2014) 1-6.
[14] Recep Calin, Muharrem Pul, Zühtü Onur Pehlivanli, Materials Research, 15, 6, (2012), 1057-1063.
[15] Luo, Z.P., Acta Materialia, 54, 1 (2006).
[16] Bowen Xiong, Qingsong Yan, Baiping Lu, Changchun Cai, Journal of Alloys and Compounds, 509 (2011) 1187-1191
[17] Z. Chen, Chemical Thermodynamics of Refractories, p. 565. Metallurgical Industrial Publishing, Beijing, 2005.
[18] L. A. Dobrzański, K. Labisz, A. Olsen, Journal of Achievements in Materials and Manufacturing Engineering, 26, 2, February (2008).